Energy, Mines and Resources Canada | Énergie, Mines et Ressources Canada

CANMET

Canada Centre for Mineral and Energy Technology | Centre canadien de la technologie des minéraux et de l'énergie

GAMMA-RAY METHODOLOGY FOR THE DETERMINATION OF LEAD-210 IN MINERALOGICAL MATERIALS

C.W. Smith
Chemical Laboratory

Yang Junhao
Chemical Laboratory

November 1984

Project MRP-3.8.0.1.11
Analytical Methodology
Project MRP-3.8.0.1.01
Reference Materials

MINERALS RESEARCH PROGRAM
MINERAL SCIENCES LABORATORIES
DIVISION REPORT MRP/MSL 84-147 (IR)

MICROMEDIA

FEB 27 1985

GAMMA-RAY METHODOLOGY FOR THE DETERMINATION OF LEAD-210 IN MINERALOGICAL MATERIALS

by

C.W. Smith* and Yang Junhao**

ABSTRACT

Lead-210 activities in CCRMP uranium reference materials DL-1a, BL-4a, DH-1a and BL-5 were measured from the 46.52 KeV gamma-ray photopeak intensities using a 1000 mm^2 x 5 mm intrinsic germanium detector. Calibration was performed with aliquots of ^{210}Pb certified reference material RBZ.44 adsorbed on a variety of mineralogical matrices. Data were corrected for sample-dependent dead-time and self-absorption effects on the photopeak area. Self-absorption correction was based on photopeak attenuation coefficients determined experimentally for each sample from transmission measurements with a 74 kBq ^{210}Pb source, assuming a simple exponential attenuation law applies. Results were in good agreement with those obtained by the method of standard additions. The activities obtained were 1.38 ± 0.05, 15.72 ± 0.33, 31.68 ± 0.58, and 862 ± 18 Bq g^{-1} respectively for the references materials, the uncertainties being 95% confidence intervals for the means of four determinations.

---

* Research Scientist, Chemical Laboratory, CANMET, Energy, Mines and Resources Canada.

**Visiting Scientist, Chemical Laboratory, 1983-4. Currently Senior Analytical Chemist, Beijing Research Institute of Uranium Geology, P.O. Box 764, Beijing, China.

DÉTERMINATION DU PLOMB-210 CONTENU DANS LES MATÉRIAUX MINÉRALOGIQUES PAR LA MÉTHODE DE RAYONNEMENT GAMMA

par

C.W. Smith* et Yang Junhao**

RÉSUMÉ

On a mesuré l'activité du plomb-210 dans les matériaux de référence d'uranium DL-1a, BL-4a, DH-1a et BL-5 du Programme canadien des matériaux de référence (PCMR) à partir des intensités de pics photoélectriques de rayons gamma 46,52 KeV, à l'aide d'un détecteur intrinsèque de germanium de 1000 mm^2 X 5 mm. L'étalonnage a été fait avec de petits échantillons de ^{210}Pb du matériau de référence RBZ,44 adsorbés sur diverses matrices minéralogiques. Les données relatives aux échantillons ont été rectifiées en fonction du temps mort et des effets d'auto-absorption sur la surface des pics photoélectriques. L'auto-absorption a été réglée d'après les coefficients d'atténuation des pics photoélectriques de chacun des échantillons déterminés de manière expérimentale à partir des mesures de transmission ayant à la source 74 kBq ^{210}Pb, suivant l'hypothèse qu'une simple équation d'atténuation exponentielle s'applique. Les résultats étaient compatibles aux résultats obtenus en utilisant la méthode des ajouts. Les activités obtenues pour les matériaux de référence étaient de 1,38 ± 0,05; 15,72 ± 0,33; 31,68 ± 0,58; et 862 ± 18 Bq g^{-1} respectivement, les incertitudes pour les moyennes de quatre dosages indiquent des intervalles de confiance de 95 %.

---

*Chercheur scientifique, Laboratoire de chimie.

**Chercheur scientifique invité, Laboratoire de chimie, 1983-1984, actuellement chimiste analyste principal, Institut de recherche sur la géologie de l'uranium de Beijing, C.P. 764, Beijing, Chine.

CONTENTS

	Page
ABSTRACT	i
RESUME	ii
INTRODUCTION	1
EXPERIMENTAL	3
DISCUSSION OF RESULTS	7
CONCLUSION	9
ACKNOWLEDGEMENT	9
REFERENCES	10

LIST OF TABLES

1.	Count data from ^{210}Pb-spiked non-radiogenic matrices	11
2.	Summary of calibration data	12
3.	Summary of counting data for lead-210 determination	13
4.	Activity results for ^{210}Pb in CCRMP materials	14
5.	Count data from ^{210}Pb-additions to CCRMP materials	15
6.	Results from linear regression analysis of ^{210}Pb additions experiments	16

LIST OF FIGURES

1.	Effect of total activity (dead-time) on ^{210}Pb photopeak area	17
2.	Features of ^{210}Pb gamma-ray spectrum: spiked and unspiked SiO_2	18
3.	Features of ^{210}Pb gamma-ray spectrum: DH-1a and BL-4a	19
4.	^{210}Pb efficiency as a function of absorption properties of samples	20

INTRODUCTION

Lead-210 (^{210}Pb) is a radioactive decay product of uranium-238 which occurs naturally in the environment at low levels of activity, and at higher levels in uranium-ore tailings and in tailings effluents which have not been treated to remove radionuclides. Lead-210 activity measurements in both solid and solution matrices are consequently important in regulatory monitoring programs, tailings treatment studies, and tailings modelling programs such as incorporated in the National Uranium Tailings Program and various studies carried out in the CANMET Minerals and ERP Research Program (ERP).

In 1984, the Canadian Certified Reference Materials Project undertook to certify uranium reference materials BL-4a and BL-5 and uranium-thorium reference materials DL-1a and DH-1a for ^{210}Pb activity by an interlaboratory measurement program in response to a need for compositional certified reference materials (CRM's) for this isotope. The work described herein was carried out as a contribution to this program, and to the Analytical Methodology Project, MRP, CANMET.

Lead-210 is normally measured indirectly by radiochemical separation and measurement of its bismuth-210 daughter isotope by β-particle counting or of its polonium-210 grand-daughter by alpha-particle spectrometry, under controlled (or sometimes predictable) conditions of activity equilibrium (1). These procedures can be labour intensive and require tracing of the overall recovery of bismuth or polonium throughout the decomposition and separation procedures for accurate measurements.

Lead-210 may also be measured directly since a 46.52 KeV gamma-ray is emitted in a constant fraction, ≈4.1%, of decay events (2). The advent of high-resolution solid-state gamma-ray detectors has made it feasible to measure the photopeak due to this emission in the presence of other gamma-active isotopes without spectral interferences. It is consequently feasible to perform simultaneous measurements of ^{210}Pb and a number of other important isotopes present in a single compositional sample directly without any radiochemical separations. The gamma-ray ^{210}Pb metrology suffers from a lower efficiency for a given sample size than either of the radiochemical methods due both to the low gamma yield of 4% (compared to 100% for β or α methodology) and to the lower detection geometry that is normally necessary in the gamma-ray source/detector arrangement. For low

activity samples this may require considerable spectral accumulation periods to obtain acceptable counting statistics. This disadvantage may be offset in whole or in part by the capability to measure larger compositional samples than would normally be practical for radiochemical treatment, the potential for multiple isotope measurements, and complete freedom from recovery losses.

Use of the low energy gamma-ray region for quantitative isotope measurement has been limited since sample self-absorption is an important parameter in determining the observed photopeak count rate for these less energetic gamma-rays. It is consequently necessary to quantitate the self-absorption effect of a particular sample or to effectively eliminate it in order to measure the activity of a low energy gamma-ray emitter such as ^{210}Pb. Elimination requires placing the analyte isotope in a matrix with identical absorbing properties to the calibration matrix (normally requiring extraction of the isotope, in which case the alternative radiochemical methods maybe preferable) - or employing the method of standard additions (requiring multiple isotope addition preparations and measurements, in which case the radiochemical methods again may be preferable).

Quantitation of the self-absorption effect requires derivation of a relationship between effective sample attenuation coefficients relevant to the experimental source/detector geometry and the effect on the observed photopeak response. While it is possible to compute such effects for a given source and detector geometry and sample composition (if known) by using published elemental attenuation coefficients, it is apparently necessary to use experimentally-determined effective photopeak attenuation coefficients, since photofractions appear to be a function of unique scattering properties of a particular sample (e.g. reference 3).

Two publications involving practical quantitation of self-absorption drew our attention (4,5). The former employs large sample/small detector geometry and derives a relationship between experimentally determined effective photopeak attenuation coefficients and the absorption assuming point detector/cone collimation geometry. The latter also employs the measurement of effective photopeak attenuation coefficients and applies a factor based on attenuation paths perpendicular to the detector. Since the latter technique seemed more appropriate to our experimental geometry, and

agreement of results with those of other radiochemical methodology was indicated, it was tested and applied in the study reported herein, with successful results.

EXPERIMENTAL

Gamma-ray measurements were made with a high-purity (intrinsic) planar germanium spectrometer (APTEC/NRD PS1005-A31C), having a 1000 mm^2 x 5 mm detector crystal and a cooled FET preamplifier. The spectrometer has a 0.38 mm beryllium window and a detector-end cap distance of 6 ± 1 mm. The detector is shielded in a 10 cm thick lead castle lined with 0.84 mm cadmium and 1.4 mm copper. Voltage pulses were amplified with a spectroscopy amplifier (Canberra 2020) operated with automatic baseline restoration and an 8 µs pulse-shaping time constant. The spectra were acquired in 4096 channels of a multichannel analyser (Canberra 85) via a 100 MHz Wilkinson ADC (Canberra 8621). Energy calibration corresponds to 0.1031 KeV/channel.

A protective polystyrene plate 0.762 mm thick was placed over the detector window for all measurements. Powder samples were packed uniformly in cylindrical aluminum caps, 6.942 cm^2 x 0.790 cm, faced with Mylar film (0.01 mm, held in place by O-rings) and mounted coaxially on the plate for gamma-ray measurements. Transmission measurements for correction of absorption effects measurements were made with a 2 µCi ^{210}Pb disc source, 2.25 cm^2, mounted coaxially on top of the aluminum sample caps. This source was prepared by coprecipitation of an aliquot of a ^{210}Pb solution CRM with 6 mg of non-radiogenic lead as the sulphate which was collected on a 4.6 cm^2 membrane filter. The filter was mounted on an aluminum disc and the exposed deposit sealed with Mylar tape. The source was then contained in a 1.5 mm thick plastic case.

Calibration sources were prepared from aliquots of volumetrically diluted solutions of ^{210}Pb certified reference material RBZ.44, solution number SO/8/54 (6). These solutions contained 0.15 M nitric acid and 100 µg/mL of non-radiogenic lead and bismuth. The half-life 22.3 ± 0.2 y was used to compute lead-210 activity at the date of measurement from the activity corresponding to the certification date, 1 May 1980.

Solid matrix calibration sources were prepared by drying a small aliquot of solution absorbed on the matrix powder in a plastic vial under a heat lamp in a fume hood until all moisture had evaporated. The powder cake was crushed in a mortar and then blended in the original vial on a mixer/mill. Weighed amounts were then transferred to sample caps. Solution sources were also prepared by transferring aliquots directly to aluminum caps that had been sprayed with acrylic plastic to inhibit acid attack. Despite this treatment, attack resulting in precipitation occurred within 24 h, and solutions were disposed after measurement.

It was observed that photopeak count rates for a fixed source decreased as the total gamma activity of the sample increased. This was attributed to amplifier pulse pile-up losses which become appreciable at higher activities, particularly with the long shaping time constant used to obtain high resolution. It was determined that the effect could be quantified with respect to the ADC-registered dead-time, which largely reflects trailing-edge pile-up with the sample activities of these experiments (7). Experimentally, the ^{210}Pb disc source was mounted coaxially 14 cm above the detector on a plastic column constructed with an annular dish.

The ^{210}Pb photopeak count rate was measured as a function of increasing amounts of thorium oxide added annularly, thereby increasing the amounts of total gamma-activity and dead-time. Empirically it was found that the effect of pile-up losses could be compensated by multiplying the observed area by the factor, F,

$$F = 1/[1-1.534 \times 10^{-4}(DT)^2]$$

where DT is the ADC-registered dead-time (%). Data are shown in Figure 1. In practice, the correction is less than 1% for dead-times up to 8%. Only in the case of measurement of undiluted BL-5 (DT ≈ 18%) did dead-times exceed this, nonetheless the correction was applied to all measurements.

The ^{210}Pb photopeak area was measured between 45.42 and 47.69 KeV (23 channels). Compton background per channel beneath the peak was determined as the average of counts in 5 channel intervals adjacent to the high and low energy side of the peak. The ^{210}Pb photopeak interval corresponds to

greater than 99.9% of the area under a Gaussian peak with the same FWHM* (e.g. 655 eV, Fig. 2A). The photopeak is near-Gaussian, e.g. in Fig. 2A FW $1_{/10}$ M/FWHM = 1.78 ± 0.6 and FW $1_{/20}$ M/FWHM = 2.09 ± .06 vs theoretical values of 1.83 and 2.08 respectively (8). The relative imprecision in the photopeak area due to counting uncertainties was estimated as:

$$2\sigma\%,A = 200(I + 10.89\beta)^{1/2}/A$$

where I is the total of counts in the photopeak and background intervals, β is the total in the background intervals and 10.89 is the peak/background channel ratio squared. The calculation is performed by ROM software within the MCA.

There is a minor contribution to the ^{210}Pb photopeak area due to ^{210}Pb in the ambient materials of the castle, spectrometer, and sample container. The count rate corresponds to 0.3 ± 0.1 Bq and 0.16 ± 0.06 Bq with 8 g samples of "non-radiogenic" silica and a gabbro rock CRM (MRG-1), respectively (Fig. 2B).

Measured photopeak areas were corrected for this background contribution. The net photopeak count rate due to the sample, O, is then given by:

$$O = F[A/t - b]$$

where F is the dead-time correction factor described above, A is the net photopeak area, t is the acquisition live-time, and b is the background photopeak count rate, $(6.5 \pm 2.5)10^{-4}$ cps. The 95% CI relative imprecision in O is estimated by statistical error propagation as:

$$2\sigma\%,O = 200\ F\ [(\sigma A)^2/t^2 + (\sigma b)^2]^{1/2}/O$$

Correction for sample self-attenuation of 46.5 KeV gamma-rays is based on the exponential attenuation model with experimentally-determined

---

*FWHM is the full width of the photopeak at one-half maximum height. FW $1_{/10}$ M and FW $1_{/20}$ m are defined analagously.

photopeak attenuation coefficients. The simplified model e.g. (9) for a fixed source geometry is:

$$O = K \cdot Bq \int_0^t \exp(-\mu x)dx = Kt \cdot Bq \, [1-\exp(-\mu t)]/(\mu t)$$

where t is the fixed source thickness, μ is the photopeak linear attenuation coefficient, Bq is the source activity, and K a proportionality constant characteristic of the detector, detector-source geometry, and particular gamma-ray source. Rearranging the integrated equation yields:

$$Bq = K'OR$$

where $K' = Kt$ and R is the self-attenuation coefficient,

$$R = \mu t/[1-\exp(-\mu t)]$$

The effective value of μt is determined from the transmission experiment for each sample (and calibration standard):

$$-\ln[(T-O)/I] = \mu t$$

where T and I are the ^{210}Pb photopeak area (cps) with the ^{210}Pb source on the sample and empty sample cap respectively (5). Experimentally R is then:

$$R = -\ln[(T-O)/I]/[1-(T-O)/I]$$

The imprecision in the ratio (T-O)/I is estimated by propagation of the component counting statistics errors, and that in R was estimated from the calculated value at the 95% CI limits of the intensity ratio.

The calibration constant K' was evaluated as the mean for a number of spiked matrices (Tables 1 and 2, Figure 4):

$$K' = \sum_i^n (Bq/OR)_i/n = 193.0 \pm 2.7 \quad Bq/cps$$

The activity of a sample, j of mass W_j, is then

$$(Bq \cdot g^{-1})_j = 193 \times O_j \times R_j / W_j$$

with estimated imprecision at the 95% confidence level of:

$$2\sigma_j(\%) = [(2\sigma\%,O)^2 + (2\sigma\%,R)^2 + 1.4^2]1/2$$

Count data for the CCRMP materials are compiled in Table 3. Activity results are summarized in Table 4.

In addition to the activity measurements with experimental correction for absorption effects, the activities in the four CCRMP materials were also measured by internal standardization, employing the method of standard additions. At the expense of the additional labour involved in quantitatively spiking and then homogenizing the samples, the advantages of freedom from both variable matrix absorption and variable dead-time effects are obtained. Spiking was performed as described above for other minerals matrices. Count data for the additions experiments are in Table 5. While unnecessary for the additions results, transmission experiments were carried out so that the ore matrices could be included in calibration of self-absorption effects. Results of the regression analysis are shown in Table 6.

DISCUSSION OF RESULTS

The activity measurements of ^{210}Pb-spiked non-radiogenic matrices indicate that the photopeak area is a linear function of activity from zero to 6000 Bq for a given matrix and packing density, (Tables 1 and 2). Relative standard deviations of the photopeak count rate per becquerel from mean values were about 1% for the silica matrix, prepared by successive weight dilutions, and 2.3% for the MRG-1 matrix, prepared by separate preparations of individual aliquots. MRG-1 is a gabbro rock reference material having ^{210}Pb activity below our detection limit (10). Photopeak efficiencies for the radioactive ores were obtained from the slopes of standard additions experiments (Table 6). Imprecisions, estimated from

worst-slopes obtained from 95% confidence limit values of individual sample peak areas, were less than 1%.

There is a strong and regular dependence of the ^{210}Pb photopeak efficiency on the absorption properties of the matrix as expected (Figure 4). A regression fit of the efficiency data yields the curve indicated in Figure 4:

$$10^3.O/Bq = 4.828(1/R) + 0.234; \quad \text{correlation coefficient } 0.9936.$$

This is essentially consistent with the model for the absorption effect since the 95% confidence interval for the intercept value is ±0.21 assuming random distribution of the data (8). The 95% confidence interval for the slope value is ±6.0%. The upper data in Figure 4 shows the absorption-normalized efficiency as a function of the absorption parameter. Linear regression analysis yields the relationship:

$$10^3.OR/Bq = 0.198\ (R) + 4.88; \text{ correlation coefficient } 0.51.$$

The 95% confidence intervals for the slope and intercept respectively are ±0.15 and ±0.23, so there may be a slight residual dependence on absorption not accomodated by the model. Constraining the data to the model (zero slope) yields $10^3.OR/Bq = 5.18$ with a 95% confidence interval for the mean of ±1.4%. This value, corresponding to the efficiency at R = 1.5, with the regression fit was used to define the calibration factor for measurements of the CCRMP samples.

The analytical results are presented in Table 4. In each case, the ^{210}Pb activities are within 95% confidence interval uncertainties of agreement with activities predicted from uranium certified values assuming secular equilibrium in the ^{238}U decay series; 1.432 ± 0.037, 15.41 ± 0.09, 32.46 ± 0.04, and 87.5 ± 3.7 respectively for DL-1a, BL-4a, DH-1a and BL-5 (11). Precision estimates do not include the total uncertainty of the calibration solution, estimated as ±2.4% (6). The agreement between ^{210}Pb activity values for undiluted 8 g samples of BL-5 (DT = 18%, R = 2.3) and the diluted 1.5 g samples (DT = 3%, R = 1.4) indicates the dead-time and self-absorption corrections employed are quantitatively useful. The utility of the absorption correction parameter is further demonstrated by comparison of the results to those obtained by linear regression analysis

of standard additions experiments (Table 6). The values are identical within the 95% confidence level uncertainty estimates, with no general methodological bias being apparent.

CONCLUSION

The gamma-ray self-absorption correction technique applied herein is shown to be practical and sufficiently accurate for quantitative measurements of low-energy gamma-ray emitting isotopes in a broad range of mineral matrices with the measurement geometry used. Results are entirely consistent with those obtained by standard additions technique where the matrix-effect of self-absorption is nullified. The absorption correction technique has previously been shown to yield results in agreement with radiochemical procedures for ^{210}Pb in sediment samples in the range 0-2 Bq/g (5). Results herein were submitted as a contribution to an interlaboratory program to certify activities of ^{210}Pb in DL-1a, DH-1a, BL-4a, and BL-5, which will provide more data to compare gamma-ray and radiochemical methodologies (12). The gamma-ray method for ^{210}Pb may be competitive with labour-intensive radiochemical methods for samples of sufficient activity.

ACKNOWLEDGEMENT

This work was carried out in contribution to the "Analytical Methodology" and "Reference Materials" Project (3.8.0.1.11 and 3.8.0.1.01) of the Minerals Research Program, CANMET.

REFERENCES

1. Smithson, G.L., Dalton, J.L. and Mason, G.L. "Radiochemical procedures for the determination of selected members of the uranium and thorium series"; CANMET Report 78-22, CANMET, Energy, Mines and Resources Canada; 1979.
2. Heath, R. "Gamma-ray energies and intensities of radionuclides" In: CRC Handbook of Chemistry and Physics, 62nd Ed.; CRC Press, Boca Raton; 1981.
3. Kaplanis, S.N. "On the photofraction correction for voluminous sources and the mean photon path"; Int J Appl Radiat Isot 33:605-611; 1982.
4. Ostrihansky, L. "Radioactive disequilibrium investigations, Elliot Lake area, Ontario"; Geol Surv Can Paper 75-38; Geological Survey of Canada; 1976.
5. Cutshall, N.H., Larsen, I.L. and Olsen, C.R. "Direct analysis of ^{210}Pb in sediment samples: self-absorption corrections"; Nucl Instr Meth 206:309-312; 1983.
6. Amersham International Ltd. "Certificate of measurement of and purity of absolutely standardized radioactive solution; certificate P18537, product RBZ.44, solution number SO/8/54"; Amersham U.K.
7. Canberra Industries Ltd. "Operating manual, model 8621 ADC/SCA"; Meriden Conneticut; 1980.
8. Lark, P.D., Craven, B.R. and Bosworth, R.C. "The handling of chemical data"; Permagon Press, Oxford; 1968.
9. Price, W.J. "Nuclear radiation detection"; McGraw-Hill, New York; 130-132; 1958.
10. Abbey, S. "Reference materials - rock samples SY-2, SY-3, MRG-1"; CANMET Report 79-35, CANMET, Energy, Mines and Resources Canada; 1979.
11. Smith, C.W. and Steger, H.F. "Radium-226 in certified uranium reference ores DL-1a, BL-4a, DH-1a and BL-5"; CANMET Report 83-9E, CANMET, Energy, Mines and Resources Canada; 1983.
12. Smith, C.W. and Steger, H.F. "Lead-210 in certified uranium reference ores DL-1a, BL-4a, DH-1a and BL-5; CANMET Report to be published 1984.

Table 1 - Count data from ^{210}Pb-spiked "non-radiogenic" matrices. Count rates are shown wth propagated two sigma counting statistics errors as a percentage shown in brackets.

Material	Mass (g)	^{210}Pb (Bq)	O		$\frac{T-O}{I}$	R	OR	
0.15 M HNO_3	5.48	137.	.630	(1.1)	.8192 (.39)	1.103 (2.6)	.695	(2.8)
	5.43	910.9	4.15	(.78)	.8301 (.58)	1.096 (4.2)	4.55	(4.3)
	5.43	9109.	41.4	(.43)	.8361 (.46)	1.092 (3.5)	45.7	(3.5)
Silica	8.12	0.	0(.0012±38%)		.6619 (.51)	1.220 (1.6)	-	
	8.04	13.16	.0550	(2.3)	.6573 (.57)	1.224 (1.7)	.0673	(2.9)
	7.90	99.1	.421	(.87)	.6666 (.57)	1.216 (1.8)	.512	(2.0)
	8.06	211.2	.878	(.85)	.6601 (.57)	1.222 (1.8)	1.073	(2.0)
	8.09	423.9	1.80	(1.1)	.6503 (.57)	1.230 (1.7)	2.209	(2.0)
	7.92	829.6	3.51	(.45)	.6543 (.58)	1.227 (1.8)	4.304	(1.9)
	8.01	1678.	7.02	(.75)	.6530 (.59)	1.228 (1.8)	8.621	(1.9)
	7.70	3226.	13.80	(.85)	.6796 (.60)	1.206 (2.0)	16.64	(2.2)
	7.01	5877.	25.16	(.55)	.6948 (.63)	1.193 (2.2)	30.02	(2.3)
MRG-1		0.	0(.00065±38%)				-	
	7.64	15.34	.0567	(2.1)	.4168 (.71)	1.501 (.96)	.0851	(2.3)
	7.80	104.6	.367	(.86)	.4089 (.65)	1.513 (.86)	.555	(1.2)
	7.57	1015.	3.60	(.45)	.4127 (.67)	1.507 (.89)	5.42	(1.0)
	7.65	1025.	3.72	(1.1)	.4124 (.67)	1.507 (.89)	5.60	(1.4)
	7.68	1030.	3.61	(.45)	.4082 (.44)	1.514 (.38)	5.47	(.73)
	8.07	1074.	3.76	(.45)	.4242 (.67)	1.489 (.92)	5.61	(.10)
	8.07	1074.	3.74	(.75)	.4135 (.67)	1.506 (.89)	5.63	(1.2)
	8.07	1074.	3.73	(.45)	.4246 (.67)	1.489 (.93)	5.55	(1.0)
	6.78	5725.	20.2	(.45)	.4568 (.64)	1.442 (.98)	29.09	(1.1)
	7.09	5990.	20.6	(1.0)	.4264 (.77)	1.482 (1.1)	30.61	(1.5)
UO_3/SiO_2 (5%)	7.99	2645.	8.35	(.85)	.3389 (.66)	1.637 (.70)	13.67	(1.1)
UO_3/SiO_2 (10%)	8.00	2642.	6.62	(.55)	.1757 (.81)	2.110 (.50)	13.96	(.74)

Table 2 - Summary of calibration data. Values in brackets are the relative standard deviation (%) of the n determinations from the mean values indicated.

Matrix	n	$\overline{R}$	$10^3\overline{O/Bq}$	$10^3.\overline{OR/Bq}$
0.15 M HNO_3	3	1.097 (.51)	4.560 (.37)	5.021 (.56)
Silica	8	1.218 (1.05)	4.226 (1.11)	5.145 (.85)
DL-1a	4	1.222 (.41)	4.172 (.55)	5.098 (.69)
BL-4a	4	1.319 (.30)	3.927 (.43)	5.180 (.52)
BL-4	4	1.320 (.20)	3.992 (.58)	5.269 (.61)
DH-1a	4	1.332 (.49)	3.846 (.57)	5.122 (.75)
	4	1.414 (.58)	3.569 (.52)	5.046 (.78)
MRG-1	9	1.501 (.77)	3.531 (2.31)	5.301 (2.60)
5% UO_3/SiO_2*	1	1.637 (.44)	3.158 (.85)	5.169 (.96)
10% UO_3/SiO_2	1	2.110 (.28)	2.501 (.55)	5.178 (.62)
BL-5**	2	2.310 (.43)	2.312 (.67)	5.341 (.80)
			Mean:	5.179
			RSD:	2.05%
			95% CI, mean %:	1.38%

* (95% CI), counting statistics
**error estimates from 95% CI "worst" slopes

Table 3 - Summary of counting data for lead-210 determination. Count rates (cps) are shown with progagated two sigma counting statistics errors shown as a percentage in brackets

Material	Mass (g)	O	(T-O)/I	R	OR
DL-1a	6.979	.0391 (4.2)	.636 (.53)	1.244 (1.5)	.0486 (4.5)
	7.232	.0407 (3.5)	.629 (.51)	1.250 (1.4)	.0509 (3.8)
	7.059	.0412 (3.9)	.634 (.57)	1.245 (1.6)	.0513 (4.2)
	6.914	.0404 (4.1)	.642 (.57)	1.238 (1.6)	.0500 (4.4)
BL-4a	7.354	.4549 (1.6)	.550 (.65)	1.329 (1.3)	.604 (2.1)
	7.430	.4510 (1.7)	.551 (.65)	1.328 (1.4)	.599 (2.2)
	7.670	.4607 (1.8)	.532 (.65)	1.348 (1.3)	.621 (2.2)
	7.558	.4632 (1.8)	.540 (.65)	1.340 (1.3)	.621 (2.2)
DH-1a	6.551	.7874 (1.5)	.518 (.57)	1.364 (1.1)	1.074 (2.0)
	6.502	.7854 (1.5)	.522 (.61)	1.360 (1.2)	1.068 (1.9)
	7.090	.8450 (1.5)	.496 (.71)	1.391 (1.2)	1.175 (1.9)
	6.959	.8283 (1.5)	.517 (.66)	1.366 (1.2)	1.132 (1.9)
BL-5/SiO_2 (5:25 w/w)	7.475	4.03 (1.1)	.519 (.65)	1.363 (1.2)	5.495 (1.6)
	7.524	4.06 (.7)	.511 (.67)	1.373 (1.2)	5.573 (1.4)
	7.774	4.18 (1.2)	.503 (.67)	1.383 (1.2)	5.781 (1.7)
	7.020	3.92 (.7)	.533 (.58)	1.347 (1.1)	5.282 (1.6)
BL-5	7.665	15.14 (1.0)	.142 (1.5)	2.275 (.81)	34.44 (1.3)
	8.040	15.28 (1.0)	.129 (1.0)	2.351 (.51)	35.92 (1.1)
	8.114	15.47 (1.0)	.129 (1.1)	2.351 (.56)	36.36 (1.1)
	8.066	15.50 (1.0)	.133 (.89)	2.326 (.46)	36.05 (1.1)

Table 4 - Activity results for ^{210}Pb in CCRMP uranium reference materials from gamma-ray spectrometry measurements at 46.5 KeV

Material	Bq/g Found (±95% CI)	Mean (±95% CI)
DL-1a	1.344 ± .063 1.358 ± .055 1.402 ± .062 1.396 ± .064	1.375 ± .049
BL-4a	15.85 ± .40 15.56 ± .40 15.62 ± .41 15.86 ± .41	15.72 ± .33
DH-1a	31.64 ± .73 31.70 ± .75 31.98 ± .76 31.39 ± .74	31.68 ± .58
BL-4 (diluted)	851.2 ± 18.2 857.6 ± 16.8 861.0 ± 18.8 871.1 ± 16.5	860.2 ± 17.8
BL-5	867.1 ± 16.4 862.2 ± 15.3 864.8 ± 15.5 862.5 ± 15.2	864.1 ± 12.5

Table 5 - Count data from ^{210}Pb additions experiments. Count rates (cps) are shown with propagated two sigma uncertainty estimate as a percentage in brackets.

Material	Mass (g)	Addition (Bq)	0	$\frac{T-0}{I}$	R
DL-1a	6.996	0	0.0412 (3.8)	.6598 (.52)	1.222 (1.61)
	6.999	34.72	0.1858 (2.2)	.6669 (.62)	1.216 (1.97)
	6.999	117.0	0.5352 (1.3)	.6598 (.57)	1.222 (1.76)
	6.998	231.9	1.007 (1.4)	.6529 (.50)	1.228 (1.50)
BL-4a	7.500	0	0.4558 (1.6)	.5615 (.71)	1.316 (1.53)
	7.501	125.3	0.9453 (0.9)	.5585 (.65)	1.319 (1.39)
	7.500	248.2	1.439 (.7)	.5604 (.64)	1.317 (1.37)
	7.501	497.1	2.406 (.7)	.5532 (.72)	1.325 (1.51)
BL-4	7.499	0	0.596 (1.9)	.5521 (.57)	1.326 (1.19)
	7.497	125.1	1.100 (1.1)	.5613 (.57)	1.316 (1.23)
	7.498	248.5	1.577 (1.5)	.5555 (.57)	1.323 (1.20)
	7.499	498.6	2.589 (1.1)	.5631 (.58)	1.315 (1.26)
DH-1a	6.520	0	0.7875 (1.7)	.5511 (.52)	1.327 (1.08)
	6.512	109.9	1.215 (1.1)	.5439 (.57)	1.335 (1.16)
	6.514	216.9	1.630 (1.6)	.5515 (.43)	1.327 (.90)
	6.520	327.8	2.047 (1.5)	.5392 (.58)	1.340 (1.16)
DH-1a	8.214	0	0.9311 (1.3)	.4724 (.55)	1.421 (.88)
	8.212	139.1	1.420 (.98)	.4805 (.49)	1.419 (.81)
	8.219	275.6	1.906 (1.0)	.4855 (.36)	1.404 (.60)
	8.224	413.6	2.408 (1.2)	.4777 (.46)	1.421 (.75)
BL-5	8.251	0	15.73 (.85)	.1360 (1.96)	2.309 (1.03)
	8.253	6885	31.64 (.25)	.1357 (.47)	2.311 (.25)

Table 6 - Results from linear regression analysis of ^{210}Pb additions experiments

Parameter	DL-1a	BL-4	BL-4a	DH-1a(A)*	DH-1a(B)*	BL-5
Cor. Coef. :	.999935	.999933	.999964	.999935	.999946	-
10^3 Slope (b): (cps/Bq)	4.1722	3.9917	3.9272	3.8459	3.5690	2.312
Intercept (a):	.041917	.59510	.45686	.79060	.92731	15.73
$10^3.S_e$:	4.0916	8.5285	6.1446	5.3208	5.6971	-
$10^5.S_b$:	2.2915	2.3141	1.6728	2.1825	1.8499	(1.55)**
$10^3.S_a$:	3.0025	6.6064	4.7631	4.4536	4.7739	(67.)**
Bq @ 0 addition :	10.05	149.1	116.3	205.6	259.8	6805.9
Bq/g :	1.436	19.88	15.51	31.55	31.65	824.9
±95% CI*** :	±.444	±1.07	±.754	1.09	.994	(56.4)**

* (A) 6.52 g measurements
(B) 8.22 g measurements

** estimated from worst fit data at 95% CI limits for counts
***Bq at zero addition = a/b; $s(\%) = (S_a(\%)^2 + S_b(\%)^2)^{1/2}$, $t_{.05,2} = 4.30$

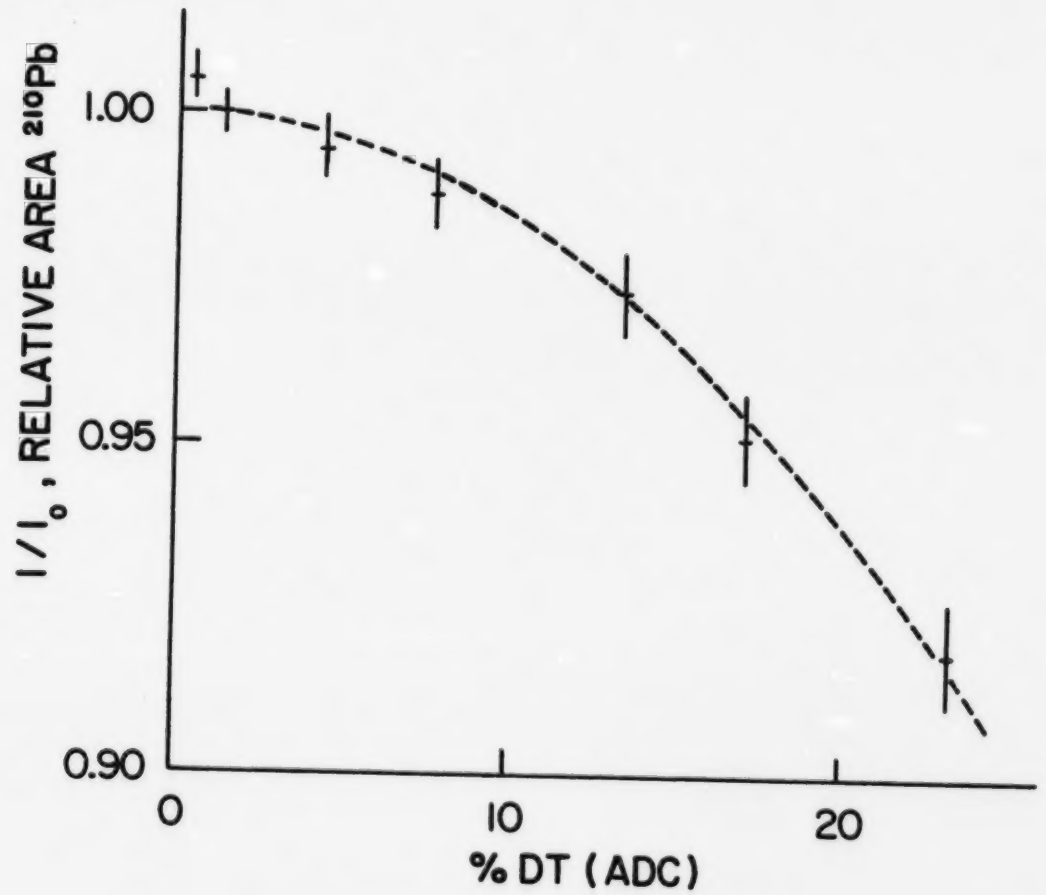

Fig. 1 - Relationship between ADC registered dead-time and measured area for a fixed ^{210}Pb source. Dashed line is result of linear regression fit of area vs DT^2, I/IO = 1-(1.534E-4)$(DT)^2$

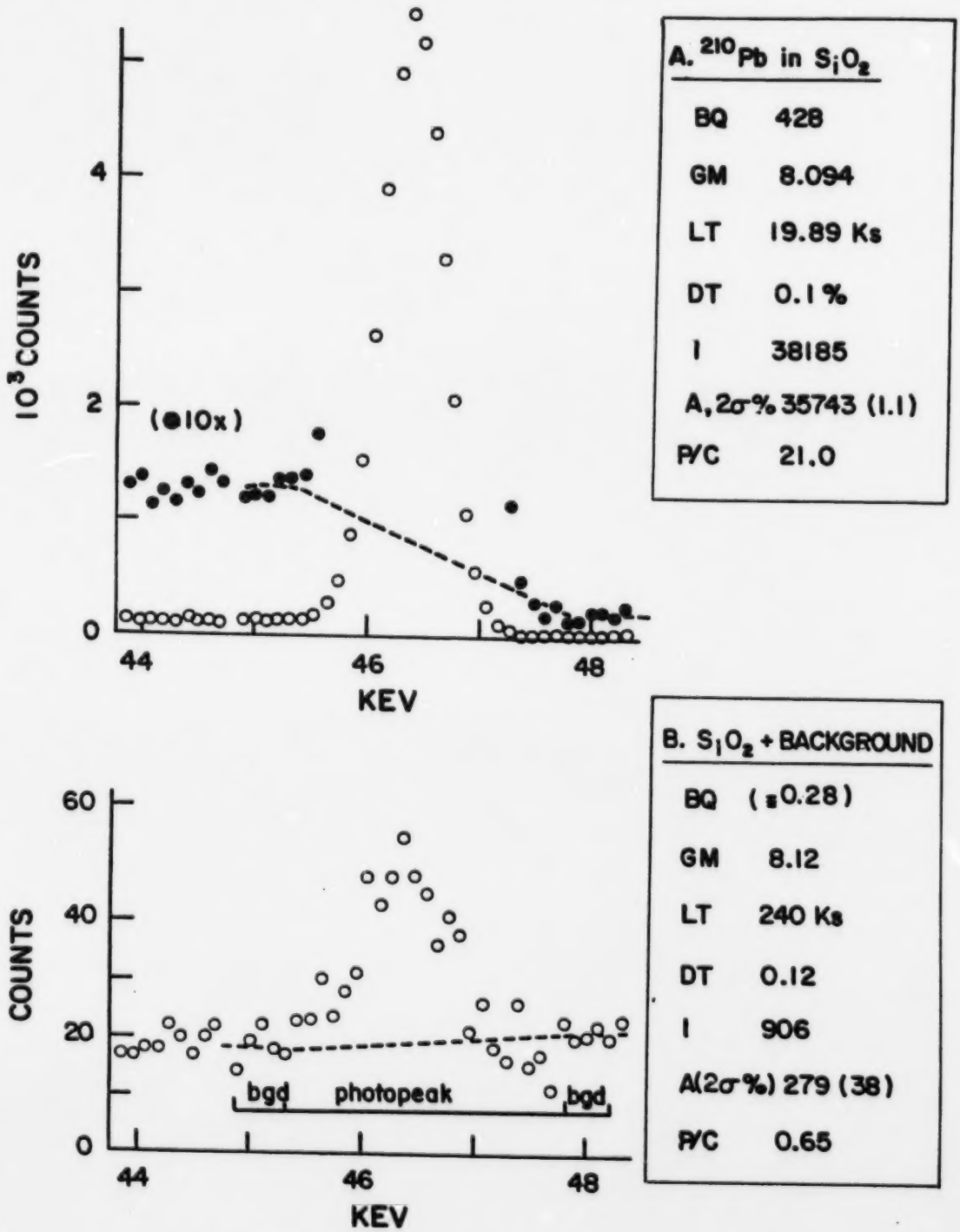

Fig. 2 - Features of ^{210}Pb gamma-ray spectra. Expanded scale shows detail of Compton background interpolation. Key: Bq = ^{210}Pb activity, GM = mass of source, LT = live-time, DT = % dead-time, I = integral counts in ROI, A = netcounts in photopeak, 2σ% = counting statistics precision of A, P/C = ratio of peak area to Compton area beneath peak

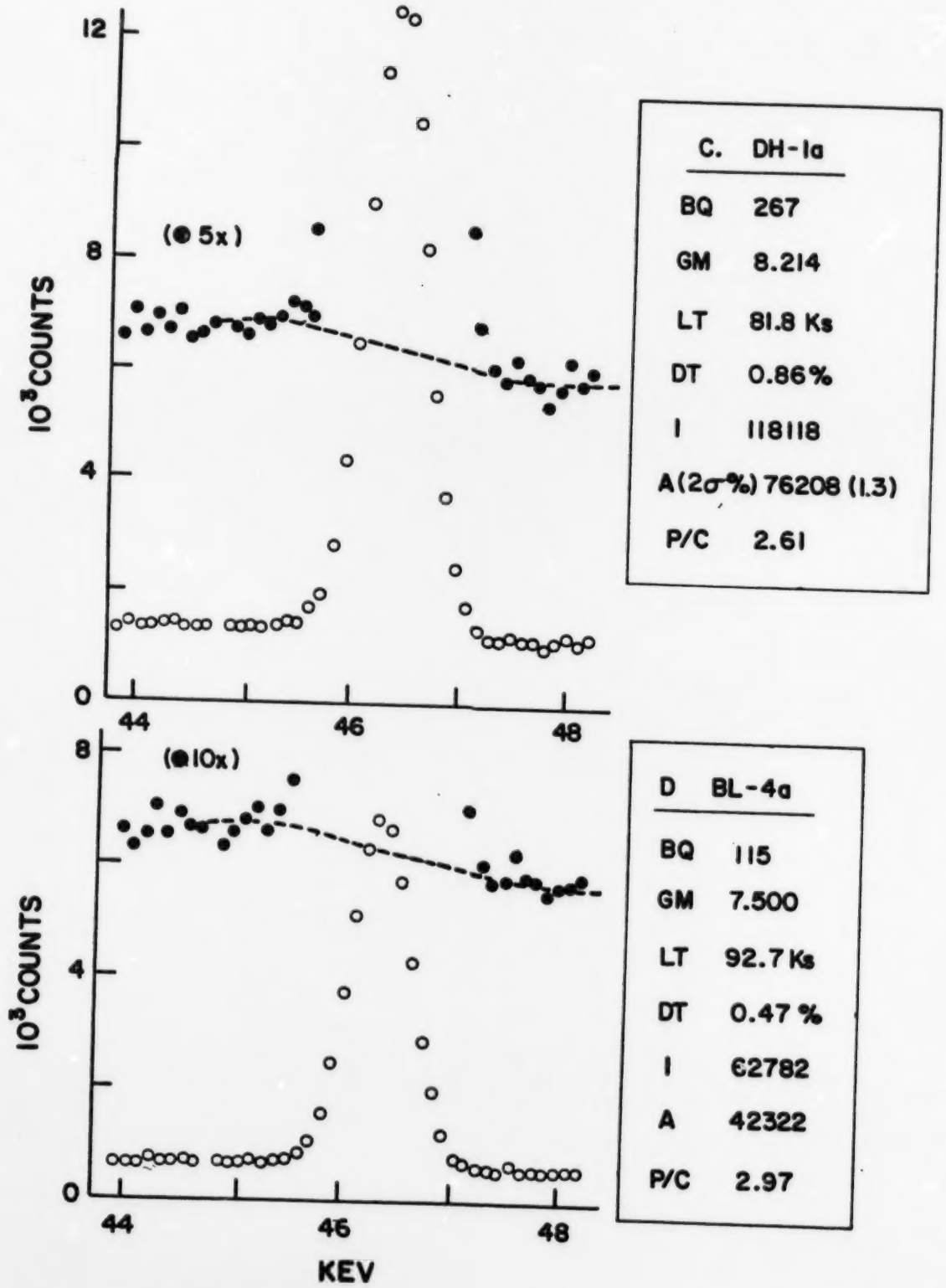

Fig. 3 - Features of ^{210}Pb gamma-ray spectra. See Fig. 1 for key

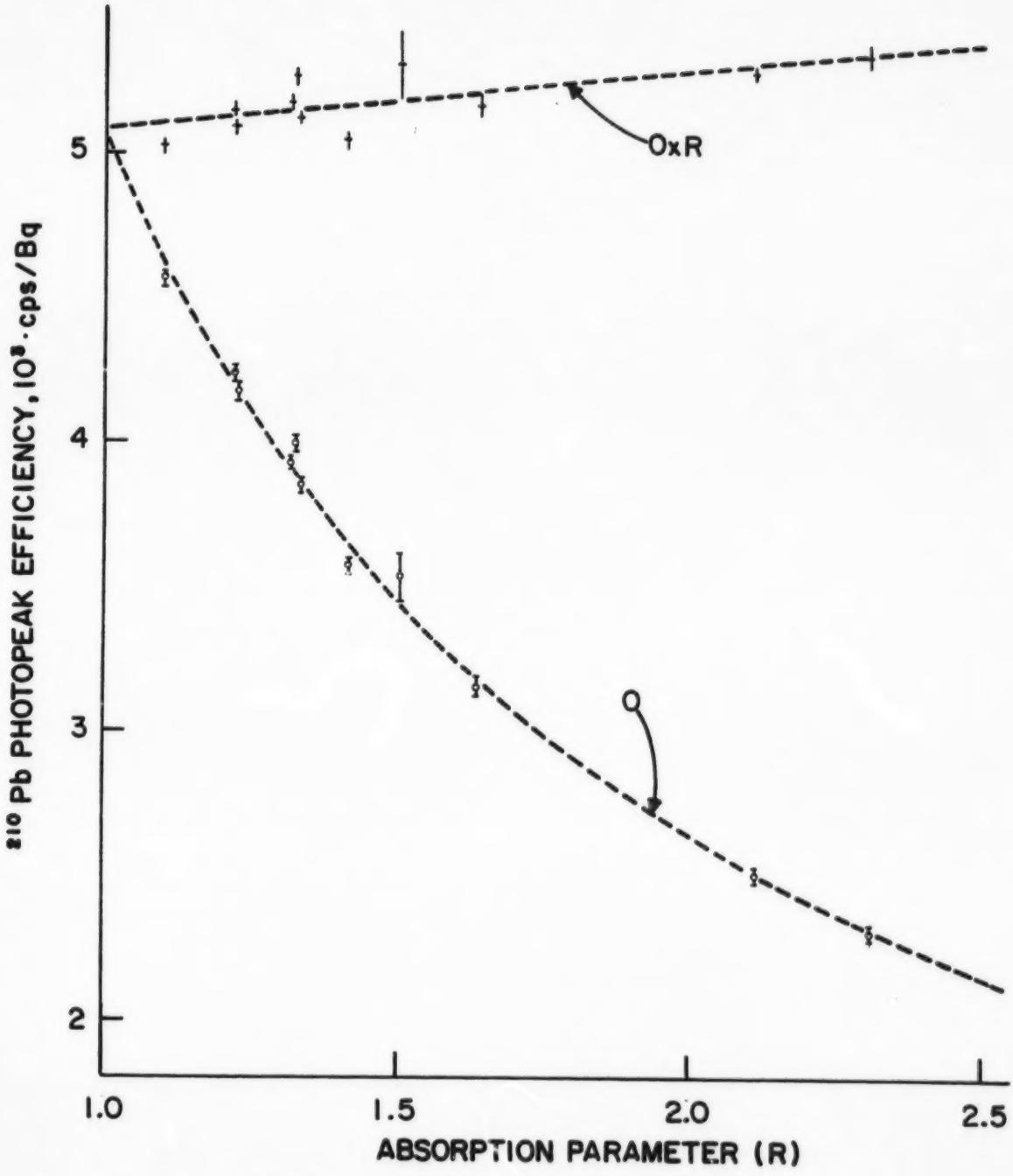

Fig. 4 - ^{210}Pb efficiency as a function of absorption properties of samples; lower no correction, upper with correction. Data from Table 2. Dashed lines are linear regression fits; O = a(I/R) + b (lower), and OR/Bq = aR + b (upper). Vertical bars are standard deviations of replicate measurements